https://doi.org/10.1007/s41230-020-9159-6

Effect of growth rate on microstructure and microhardness of directionally solidified Ti-44Al-5Nb-1.5Cr-1.5Zr-1Mo-0.1B alloy

Zhi-ping Li, Hong-ying Xia, *Liang-shun Luo, Bin-bin Wang, Liang Wang, Yan-qing Su, Jing-jie Guo, Heng-zhi Fu

National Key Laboratory for Precision Hot Processing of Metals, Harbin Institute of Technology, Harbin 150001, China

Abstract: The effect of growth rates (V=2–50 μm·s^{-1}) on microstructure and microhardness of directionally solidified Ti-44Al-5Nb-1.5Cr-1.5Zr-1Mo-0.1B (at.%) alloy at a constant temperature gradient (G=18 K·mm^{-1}) was investigated. Results indicated that β phase was the primary phase of the directionally solidified Ti-44Al-5Nb-1.5Cr-1.5Zr-1Mo-0.1B alloy. As the growth rate increases, the solid/liquid interface turns from cellular growth to dendric growth. The interlamellar spacing (λ_s) decreases with the increase of growth rate according to the relationship of λ_s=3.39$V^{-0.31}$. The solidification segregation occurs due to the enrichment of β-stabilizing element Nb, Cr in primary β phase during solidification; moreover, the degree of the segregation increases with the growth rate, resulting in the emergence of B2 phase in lamellar colonies at high growth rates. The microhardness (H_v) grows with the growth rate based on the equation of H_V=328.69$V^{0.072}$, which mainly attributes to the microstructure refinement.

Key words: beta-solidifying TiAl alloys; directional solidification; microstructure evolution; microstructure control; microhardness

CLC numbers: TG146.23 **Document code:** A **Article ID:** 1672-6421(2020)04-293-08

TiAl alloys are a kind of novel high temperature structure materials, with the promising properties of low density, high specific strength and excellent resistance to oxidation [1-4]. In the last two decades, TiAl alloys were applied in automobile industry and aerospace field as the candidate materials that replace superalloys at the working temperature of 700–1,000 °C [5-11]. However, poor room-temperature ductility of TiAl alloys, with the elongation less than 2% in general, limits its further application. Compared with other microstructures in TiAl alloys, fully lamellar structure has a better fracture toughness because the existence of interface between lamellae can stop the crack propagation [12-13]. Besides, the mechanical properties of TiAl alloys with a fully lamellar structure exhibit anisotropy at different angles between load axis and lamellar orientation, and a good balance of yield strength and elongation is able to be obtained when the angle is 0°. Thus, the mechanical properties of TiAl alloys can be enhanced by controlling the lamellar orientation using directional solidification technique [14-15]. Chen et al. [16] prepared Ti-45Al-8Nb single crystals with the lamellar orientation parallel to growth direction using the Bridgman-type directional solidification apparatus, and the mechanical properties have been enhanced significantly with the elongation of 6.9% and the yield strength of 708 MPa at room temperature. Additionally, Ti-45Al-8Nb single crystals exhibit excellent high temperature performances: a yield strength of 637 MPa and an elongation of 8.1% at 900 °C. Kartavyk et al. [17-20] has studied the microstructures and mechanical properties of β-stabilized γ-TiAl alloy Ti-44Al-5Nb-3Cr-1.5Zr by directional solidification technique. Results showed the microstructure of the β-stabilized TiAl alloys was refined after directionally solidified and B2 phase that homogeneously distributed between lamellae was decreased in volume. These improves the mechanical properties of TiAl (Nb, Cr, Zr) alloys and increases their service temperature from 750–800 °C of as-cast one to 900–950 °C of the alloy directionally solidified [17-20].

Now, adjusting solidification path and using seed materials are the two major methods to control the lamellar orientation in directionally solidified TiAl alloys. Adjusting solidification path is relatively easier

***Liang-shun Luo**

Male, born in 1980, Ph. D., Associate Professor. His research interests mainly focus on novel TiAl based alloys and directional solidification technology.

E-mail: luols@hit.edu.cn

Received: 2019-12-23; Accepted: 2020-03-05

than using seed materials to obtain well-aligned microstructure because the primary β phase that grows along the orientation of <001> is the only requirement. Then microstructure with its lamellar orientation parallel or 45° to growth direction can be obtained according to Burgers orientation relationship [21]. In order to control TiAl alloys solidifying via single β phase completely and to avoid decrease of γ/α_2 rate of lamellar structure caused by Al-lean composition, β-stabilizing elements, Mo, W, Nb, V, Cr, Ta etc. are added into TiAl alloys, which can push the β-phase region to Al-rich side [22-24]. But, the addition of a large number of β-stabilizing elements can make the solidification of TiAl alloys more complex under different cooling conditions. Jung et al. [23, 25] has studied the directionally solidified microstructure of Ti-47Al-2W and found the preferred growth direction of β phase turns <001> to <111> with the growth rates increasing from 30 mm·h^{-1} to 90 mm·h^{-1}. Xiao et al. [26, 27] has found the primary β phase of Ti-47Al-2Cr-2Nb grows along <110> instead of <001> at high temperature gradient during directional solidification.

As previously mentioned, Ti-44Al-5Nb-3Cr-1.5Zr alloy prepared by Kartavyk et al. [17-20] using directional solidification exhibits good mechanical properties but has a coarse microstructure and poor high-temperature mechanical properties. Thus, in this study, authors try to refine the microstructure and improve the high-temperature mechanical properties of the Ti-44Al-5Nb-3Cr-1.5Zr alloy by adding Mo, B and adjusting Cr content. The microstructure evolution of Ti-44Al-5Nb-1.5Cr-1.5Zr-1Mo-0.1B alloy under a constant temperature gradient during directional solidification was investigated. The effects of growth rate on the solid/liquid interface morphology, microstructure, and microhardness of directionally solidified samples were discussed. These results will contribute to control the directionally solidified TiAl alloys' microstructures which is in favour of the further application of TiAl alloys.

1 Experimental procedure

Ti-44Al-5Nb-1.5Cr-1.5Zr-1Mo-0.1B (at.%) alloy master ingot was prepared by using Ti (99.99%), Al (99.99%), Al-70wt.% Nb (commercial purity), Al-70wt.% Cr (commercial purity), Ti-40wt.% Zr (commercial purity), Ti-13wt.% Mo (commercial purity) and Al-4.8wt.% Ti-1wt.% B (commercial purity), utilizing a cold crucible induction furnace in the condition of argon atmosphere. To ensure the accuracy of the ingot composition, an X-ray fluorescence analysis apparatus, Panalytical PW4400 with measured elements from F to U, was employed, using the samples sectioned from upper, middle and lower parts of the ingot randomly. The result is shown in Table 1.

Table 1: Chemical composition of the experimental Ti-44Al-5Nb-1.5Cr-1.5Zr-1Mo-0.1B (at.%) alloy

Al	Nb	Cr	Zr	Mo	Ti
43.74	5.14	1.78	1.80	1.27	Bal.

The master ingot, prepared for directional solidification experiments was machined into cylindrical bars with a diameter of 6 mm and 100 mm length by the electric spark machine. Directional solidification experiments were conducted in a Bridgman-type vacuum furnace, as shown in Fig. 1. Machined samples were placed in an alumina tube with a length of 150 mm and external/internal diameter of 8.5 mm/7 mm. The chamber of the Bridgman-type vacuum furnace was vacuumed to 5×10^{-3} Pa and 0.05 MPa high purity argon was backfilled to prevent the evaporation of elements of the alloy. The samples were heated to 1,600 °C within 2 h to avoid the reaction between the melt and crucible and held for 0.5 h. The growth rates of the directionally solidified samples ranged from 2 μm·s^{-1} to 50 μm·s^{-1}, at a constant temperature gradient of 18 K·mm^{-1}. According to the work of Fan et al. [28, 29], the temperature gradient of the Bridgman-type vacuum furnace was measured. When the growth length of directionally solidified samples reached 40 mm, quenching process was started in order to preserve the solid/liquid interface morphology.

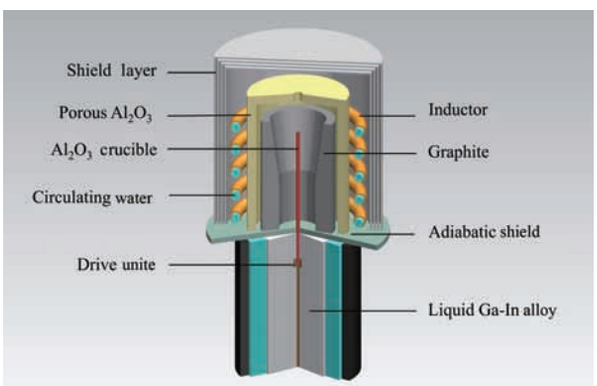

Fig. 1: Schematic diagram of the Bridgman type apparatus

The directionally solidified bars were sectioned longitudinally. The microstructures of the samples were analyzed, after being polished mechanically and etched by Kroll's solution (HF: HNO_3: H_2O = 1:1: 8, in volume), using optical microscopy and scanning electron microscopy equipped with an energy dispersive spectrometer. The average microhardness measurements were made utilizing a standardized Vickers measuring test device at a load of 9.8 N (1 kg) and a dwell time of 20 s on the surfaces of longitudinal section that were polished and slightly etched.

2 Results and discussion

2.1 Microstructure of as-cast Ti-44Al-5Nb-1.5Cr-1.5Zr-1Mo-0.1B alloy

As shown in Fig. 2, the microstructure of as-cast Ti-44Al-5Nb-1.5Cr-1.5Zr-1Mo-0.1B alloy is near lamellar structure, with a majority of ($\alpha_2+\gamma$) lamellar colonies and a few B2 phases located in the interface of lamellar colonies. Adding β-stabilizing elements such as Nb, Mo and Cr into TiAl alloys makes β phase be able to exist below the β/α transition temperature and when alloys are further cooled, disordered β phase transforms to ordered B2 structure by $\beta\rightarrow\beta_0$ reaction.

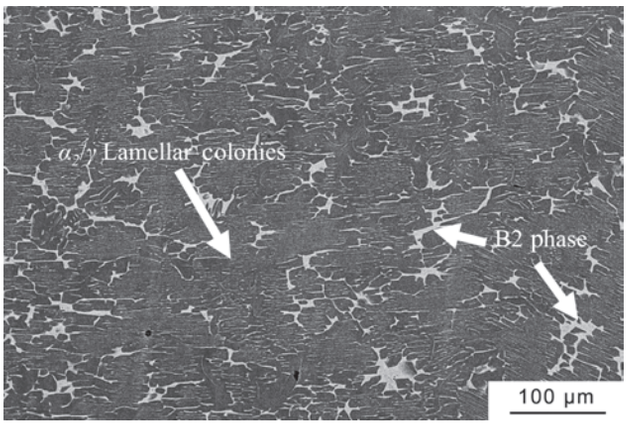

Fig. 2: Microstructure of as-cast Ti-44Al-5Nb-1.5Cr-1.5Zr-1Mo-0.1B (at. %) alloy

During the solidification of the ingot, heavy elements, Nb, Mo and Cr, which diffuse more slowly than the matrix elements Ti and Al, are enriched in the intergranular melt. This kind of segregation will result in the formation of B2 phase at the interface of lamellar colonies during the subsequent solid-state phase transformation.

2.2 Quenched solid/liquid interface and determination of primary phase

Figure 3 shows the longitudinal as-cast macrostructures of Ti-44Al-5Nb-1.5Cr-1.5Zr-1Mo-0.1B samples obtained by Bridgman-type directional solidification technique, at growth rates of 2, 5, 10, 20, 40 and 50 μm·s^{-1}, respectively.

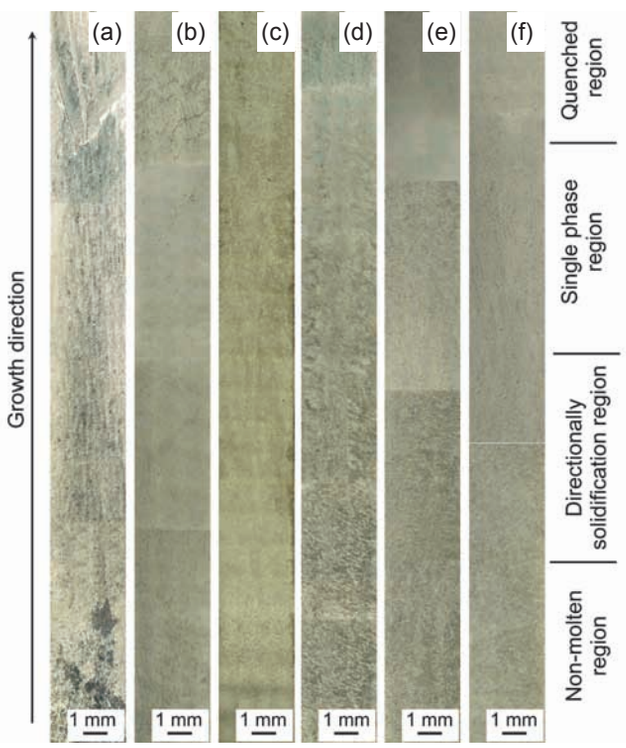

Fig. 3: Optical macrostructures of directionally solidified samples in longitudinal section at growth rate of 2 μm·s^{-1} (a), 5 μm·s^{-1} (b), 10 μm·s^{-1} (c), 20 μm·s^{-1} (d),40 μm·s^{-1} (e), and 50 μm·s^{-1} (f), respectively, under a constant temperature gradient of G=18 K·mm^{-1}

The columnar grains grow directionally and four regions could be distinguished: non-molten region, directionally solidified region, single phase region and quenched region. In non-molten region, the original as-cast microstructures are preserved because this section is placed into Ga-In alloy that prevents the alloy from melting. However, owing to the heat transfer from the melt on the top to the unmelted part in Ga-In alloy, grain boundary migration happens unidirectionally and some grains begin to grow longitudinally. The directionally solidified region consists of columnar grains with (α_2+γ) lamellar structure that come into being through solidification and a series of solid-state phase transformations. Above the directionally solidified region, single phase region is a special kind of directionally solidified region because the microstructures here are still β phase when the sample is quenched. Under a rapid cooling rate, β phase can not transform into α phase because solute atoms lack diffusion and get frozen in matrix. With further cooled, the preserved disordered β phase transforms into ordered β_0 phase with B2 structure according to order-disorder transition. So the microstructure exhibits a single β_0 phase region instead of (α_2+γ) lamellar structure. Quenched region at the top of the sample consists of columnar grains in small size which grow along the opposite direction of heat flow. The morphology of solid/liquid interface can be preserved by quenching at a high cooling rate.

Figure 4 shows the interfacial morphologies at different growth rates under a constant temperature gradient of G=18 K·mm^{-1}, with the growth direction in the figures from bottom to top. It can be seen that with the growth rates increasing, the morphologies at the solid/liquid interface change from cells [Figs. 4(a) and (b)] to dendrites [Figs. 4(c) and (d)]. Two methods have been proposed to identify the primary phase during directional solidification of TiAl alloy [32]. One is that the primary phase can be determined according to the final lamellar orientation. α or β primary phase of TiAl alloys during solidification can determine the lamellar orientation according to Burgers relationship: $\{110\}_\beta // \{0001\}_\alpha // \{111\}_\gamma$, $<111>_\beta // <11\bar{2}0>_\alpha // <110>_\gamma$. The lamellar orientation of TiAl alloys that completely solidify via β primary phase is parallel or 45° to the growth direction, while α primary phase with <0001> preferred growth direction makes the lamellar orientation perpendicular to growth direction. Another is that the primary phase can be determined by the symmetry of dendrites during solidification. Hexagonal α phase exhibits dendrites with 6-fold symmetry but cubic β phase exhibits dendrites with 4-fold symmetry. As shown in Figs. 4(c) and (d), the secondary dendrite arms are perpendicular to the primary dendrites indicating that β phase is the primary phase at the growth rates of 20 μm·s^{-1} and 50 μm·s^{-1}. Further evidence about the primary phase can be supplemented by analyzing the microstructure of directionally solidified region, as shown in Fig. 5. All the observed lamellar orientations of directionally solidified samples are parallel or 45° to the growth direction and no perpendicular lamella are detected. The orientation of lamellae formed via α primary phase can be only observed to be perpendicular to the growth

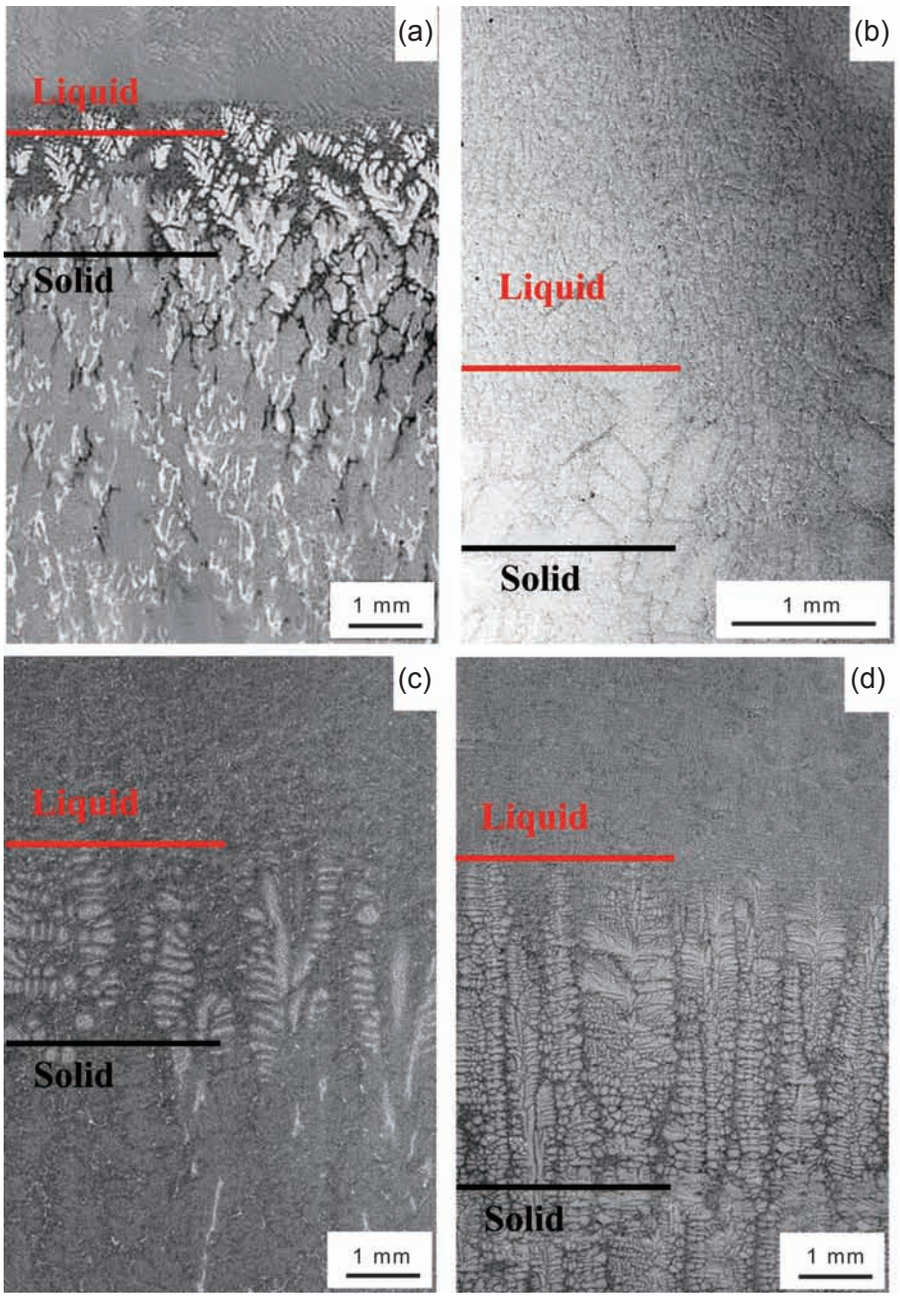

Fig. 4: Interfacial morphologies of directionally solidified Ti-44Al-5Nb-1.5Cr-1.5Zr-1Mo-0.1B alloy in longitudinal section at 2 μm·s^{-1} (a), 5 μm·s^{-1} (b), 20 μm·s^{-1} (c), and 50 μm·s^{-1} (d), respectively, under a constant temperature gradient of *G*=18 K·mm^{-1}

direction when the samples are sectioned longitudinally. Thus, the primary phase of directionally solidified Ti-44Al-5Nb-1.5Cr-1.5Zr-1Mo-0.1B alloy is β phase at the growth rates ranging from 2 μm·s^{-1} to 50 μm·s^{-1}, under a constant temperature gradient of 18 K·mm^{-1}.

2.3 Microstructures in directionally solidified region

Microstructures in the directionally solidified region are of great significance because it can evaluate the results of lamellar orientation control. The macrostructures and microstructures in the directionally solidified region are shown in Figs. 3 and 5. The directionally solidified region consists of some coarse columnar lamellar colonies which align with growth direction. At the growth rates of 2–50 μm·s^{-1}, the lamellar orientations of the directionally solidified alloys are controlled within 45° by a complete β phase solidification path according to Burgers orientation relationship. It also can be concluded from Fig. 5 that with the growth rates increasing, B2 phase begins to appear at a growth rate higher than 5 μm·s^{-1} in lamellar colonies and the interface of lamellar colonies. This appearance of B2 phase is associated with the solute segregation named S-segregation (solidification segregation) during solidification [33]. The solute distribution of dendrite and interdendrite is illustrated in Fig. 6. Because of the discrepancy of the solute distribution coefficients of each element, Al is enriched in the interdendric

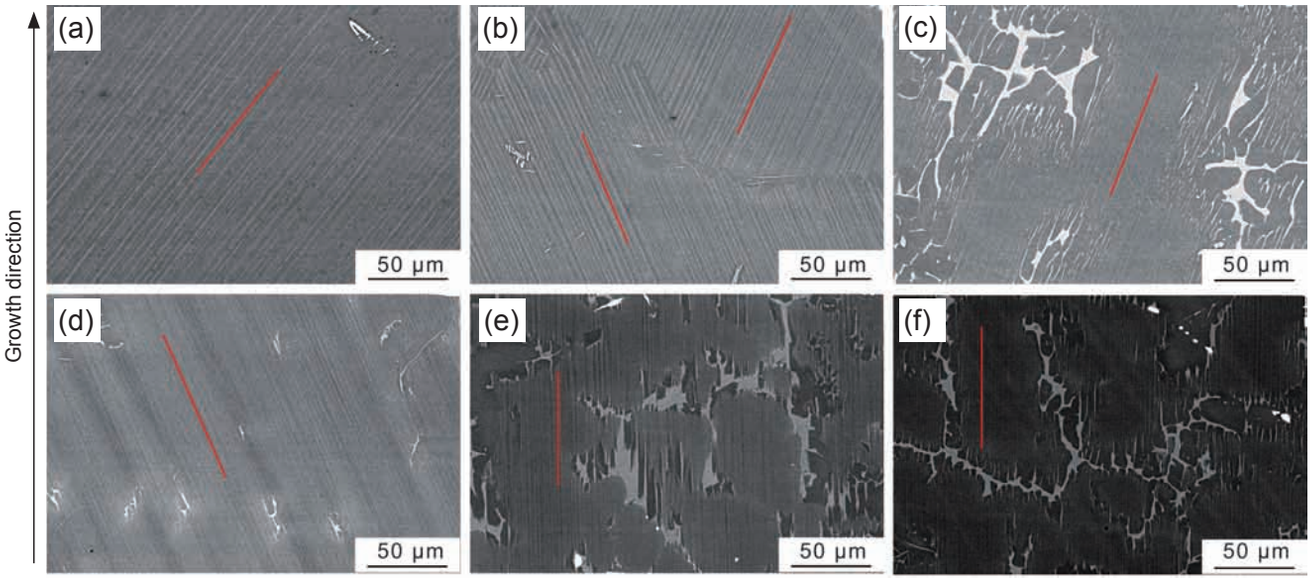

Fig. 5: Lamellar structure of directionally solidified samples at 2 μm·s^{-1} (a), 5 μm·s^{-1} (b), 10 μm·s^{-1} (c), 20 μm·s^{-1} (d), 40 μm·s^{-1} (e), and 50 μm·s^{-1} (f), respectively, under a constant temperature gradient of G=18 K·mm^{-1}

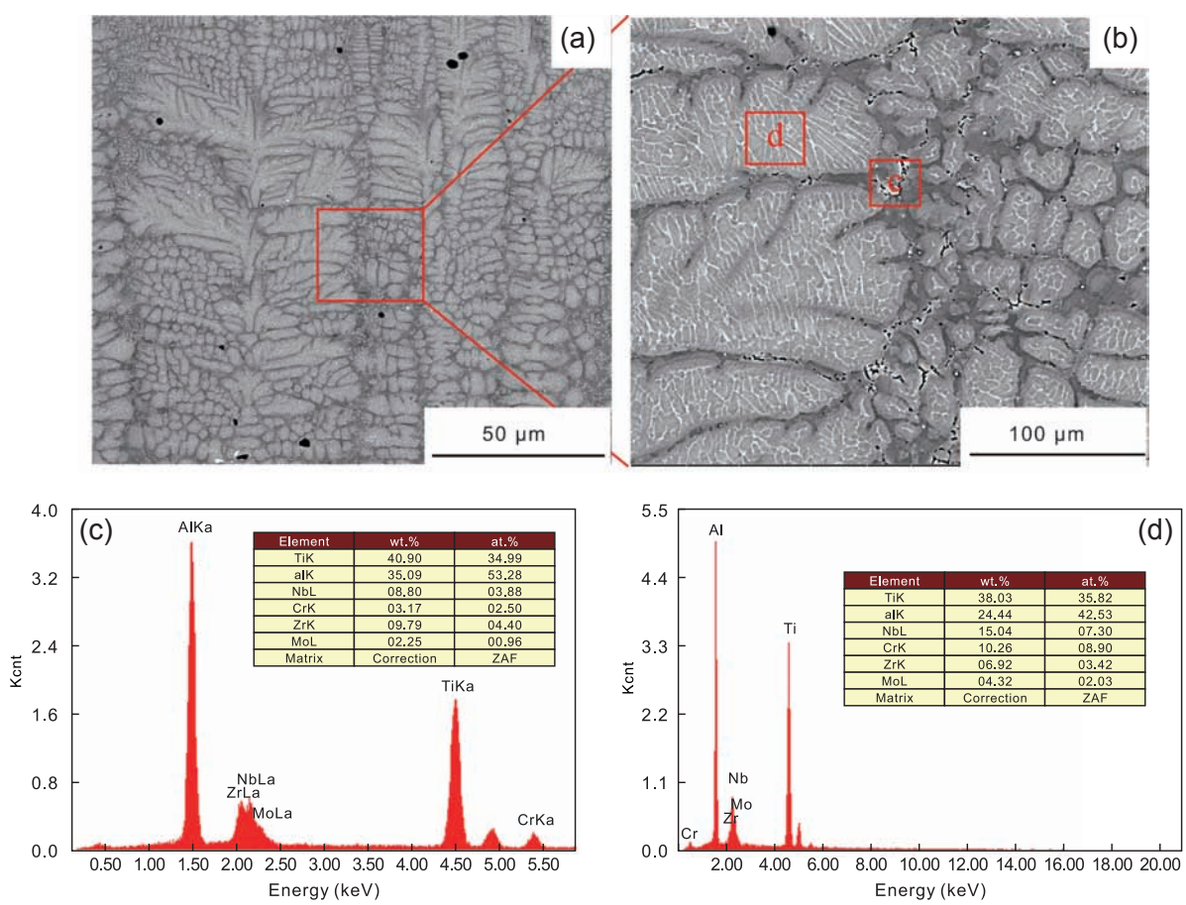

Fig. 6: Quenched solid-liquid interface morphologies in directionally solidified Ti-44Al-5Nb-1.5Cr-1.5Zr-1Mo-0.1B alloy at the growth rate of 50 μm·s^{-1} (a) and (b), and energy dispersive spectrometer (EDS) results in interdendrite (c) and dendrite (d)

region while β-stabilizing elements, Nb and Cr, are enriched in dendrites. The degree of S-segregation has a positive correlation with growth rates because Nb and Cr diffuse slowly during solidification. It makes β phase in dendric region can hardly transform into α phase via β/α transformation under subsequent cooling, and the preserved β phase turns into ordered B2 phase located in dendrites. Thus, with the increase of growth rates, B2 phase is easier to form in dendrites which is induced by a higher degree of S-segregation. It accounts for the relationship between growth rate and the distribution of

B2 phase in the directionally solidified region under a constant temperature gradient as shown in Fig. 5.

Linear intercept method [30, 31] was employed to measure the interlamellar spacing of the directionally solidified samples. Lamellar colonies of the alloys consist of platelets of γ and α_2 phases, aligned alternatively. The interlamellar spacing, defined as the width of γ+α_2 platelet unit, was obtained in BSE images of the alloys. The average values are listed in Table 2. The relationship between growth rates and interlamellar spacing was analyzed, as shown in Fig. 7. It can be concluded that the interlamellar spacing decreases with the increase of growth rate under a constant temperature gradient. The lamellar structure is obtained by a series of reaction: α→α+γ→α_2+γ. With the increase of growth rate under a constant temperature gradient, the supercooling of the solid-state phase transformation reaches a higher degree. It can increase the nucleation rate of γ phase and restrain the lateral growth of lamellae. According to current research, the relationship between interlamellar spacing (λ_s) and the growth rate (V) can be described as the following relationship [34]:

$$\lambda_s = KV^a \quad (1)$$

where K is a material constant and a is the rate exponent. Using regression analysis, the dependency of the interlamellar spacing on the growth rates (V) in the range of 2 μm·s^{-1} to 50 μm·s^{-1} can be expressed in the form of

$$\lambda_s = 3.39V^{-0.31} \quad (2)$$

Table 2: Values of lamellar spacing and microhardness for directionally solidified Ti-44Al-5Nb-1.5Cr-1.5Zr-1Mo-0.1B (at.%) alloy at various growth rates with a constant temperature gradient (G=18 K·mm^{-1})

Growth rate (μm·s^{-1})	Lamellar spacing λ_s (μm)	Microhardness (H_V)
2	2.892	347.21
5	1.806	364.12
10	1.443	391.40
20	1.516	409.35
40	1.118	426.80
50	1.074	436.50

The result is shown in Fig. 7. The regression coefficient of the fit is R^2=0.92. The exponential absolute value (0.31) is similar to the 0.32 in Ti-45Al-8.5Nb-(W, B, Y) alloy [35] and lower than the 0.94 in Ti-46Al-2Cr-2Nb-0.2B alloy [36]. Such differences may be attributed to the different compositions of alloys and solidification conditions.

2.4 Effect of growth rate on microhardness

The values of microhardness are also shown in Table 2. Microhardness is a common means to evaluate the mechanical properties of alloys. Lapin et al. [37] and Dimiduk et al. [38]

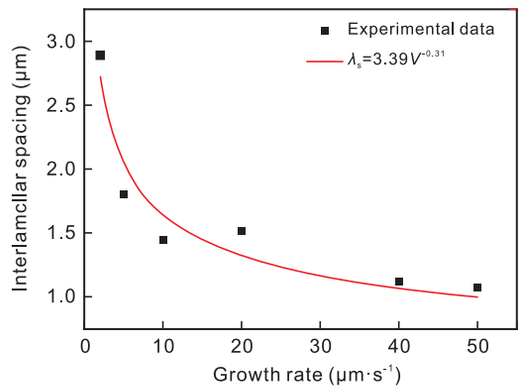

Fig. 7: Dependence of lamellar spacing (λ_s) on growth rate (V) of directionally solidified Ti-44Al-5Nb-1.5Cr-1.5Zr-1Mo-0.1B alloy under a constant temperature gradient of G=18 K·mm^{-1}

have studied directionally solidified Ti-46Al-2W-0.5Si alloy and wrought Ti-45.3Al-2.1Cr-2Nb alloy respectively, and found that there is a linear relationship between yield stress and microhardness of alloys. The relationship between microhardness (H_V) and growth rate (V) for directionally solidified TiAl alloys can be expressed with Hall-Petch type relationships as following [39]:

$$H_V = H_0 + KV^b \quad (3)$$

where b is exponent values for the growth rate (V), and H_0, K are constants which can be experimentally determined. Equation (3) can be rewritten as follows for qualitative analysis [39]:

$$H_V \approx KV^b \quad (4)$$

The relationship between H_V and V of Ti-44Al-5Nb-1.5Cr-1.5Zr-1Mo-0.1B alloy is obtained by using linear regression analysis, as shown in Fig. 8, and the result is given as follows:

$$H_V = 328.69V^{0.072} \quad (5)$$

The regression coefficient of the fit is R^2=0.99. The exponent value of growth rate (V) is 0.072, which is similar to 0.12 in Ti-50Al-6Nb alloy [40], but lower than 0.14 in Ti-46Al-2W-0.5Si alloy [37] and 0.16 in Ti-49Al alloy [28]. These difference

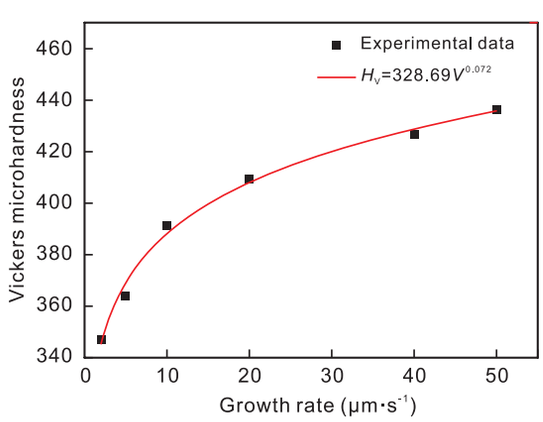

Fig. 8: Dependence of the Vickers microhardness (H_V) on the growth rate (V) in directionally solidified Ti-44Al-5Nb-1.5Cr-1.5Zr-1Mo-0.1B alloy under a constant temperature gradient of G=18 K·mm^{-1}

may be attributed to the different solidification conditions and compositions, because microhardness is sensitive to chemical composition, solidification processing parameters, and microstructures (primary dendritic spacing, lamellar spacing). Compared with the microhardness of as-cast Ti-44Al-5Nb-1.5Cr-1.5Zr-1Mo-0.1B alloy, 310–330 H_V, the microhardness of directionally solidified samples has been enhanced evidently. And with the growth rate increasing, the microhardness of directionally solidified Ti-44Al-5Nb-1.5Cr-1.5Zr-1Mo-0.1B alloy grows in accordance with Eq. (5) in general, indicating the increase of growth rate can promote the hardness by refining the lamellar structure of Ti-44Al-5Nb-1.5Cr-1.5Zr-1Mo-0.1B alloy.

3 Conclusions

The effect of growth rate on the microstructure and microhardness of Ti-44Al-5Nb-1.5Cr-1.5Zr-1Mo-0.1B alloy were studied under a constant temperature gradient of G=18 K·mm^{-1}. Results can be concluded as following:

(1) The β phase is the primary phase in directionally solidified Ti-44Al-5Nb-1.5Cr-1.5Zr-1Mo-0.1B alloy with the growth rate ranging from 2 μm·s^{-1} to 50 μm·s^{-1}. The solid/liquid interface exhibits a cellular morphology at low growth rates (≤5 μm·s^{-1}) and it changes to dendritic growth with growth rates increasing over 5 μm·s^{-1}.

(2) Lamellar structures with the angle between its orientation and growth direction less than 45° are obtained at 2 μm·s^{-1} to 50 μm·s^{-1}. B2 phase appears in (α_2+γ) lamellar colonies at high growth rates (≥ 10 μm·s^{-1}) owing to the appearance of S-segregation. The lamellar spacing decreases with the growth rate increasing according to $\lambda_s=3.39V^{-0.31}$.

(3) The microhardness increases with growth rate according to $H_V=328.69V^{0.072}$.

Acknowledgements

This research was financially supported by the National Key Research and Development Program of China (Grant No. 2016YFB0301201), National Natural Science Foundation of China (Grant Nos. 51671073, 51425402), Fundamental Research and Development Program of China (Grant No. JCKY2017205B032), Yunnan Rare Metal Materials Genetic Engineering Project (Grant No. 2018ZE013) and Major Special Science and Technology Project of Yunnan Province (Grant No. 2019ZE001).

References

[1] Yang R. Advances and challenges of TiAl base alloys. Acta Metallurgica Sinca, 2015, 2: 129–147. (In Chinese)
[2] Gupta R K, Pant B, Sinha P P. Theory and practice of γ+α_2 Ti aluminide: a review. Transactions of the Indian Institute of Metals, 2014, 67(2): 143–165.
[3] Clemens H, Mayer S. Design, processing, microstructure, properties, and applications of advanced intermetallic TiAl alloys. Advanced Engineering Materials, 2013, 15(4): 191–215.
[4] Wei D, Koizumi Y, Nagasako M, et al. Refinement of lamellar structures in Ti-Al alloy. Acta Materialia, 2017, 125:81–97.
[5] Clemens H, Mayer S. Intermetallic titanium aluminides in aerospace applications-processing, microstructure and properties. Materials at High Temperatures, 2016, 33(4–5): 560–570.
[6] Kastenhuber M, Rashkova B, Clemens H, et al. Effect of microstructural instability on the creep resistance of an advanced intermetallic γ-TiAl based alloy. Intermetallics, 2017, 80: 1–9.
[7] Wu X. Review of alloy and process development of TiAl alloys. Intermetallics, 2006, 14(10–11): 1114–1122.
[8] Appel F, Clemens H, Fischer F D. Modeling concepts for intermetallic titanium aluminides. Progress in Materials Science, 2016, 81: 55–124.
[9] Dimiduk D M. Gamma titanium aluminide alloys-an assessment within the competition of aerospace structural materials. Materials Science & Engineering: A, 1999, 263(2): 281–288.
[10] Bewlay B P, Nag S, Suzuki A, et al. TiAl alloys in commercial aircraft engines. Materials at High Temperatures, 2016, 33(4–5): 549–559.
[11] Janschek P. Wrought TiAl blades. Materials Today-Proceedings, 2015, 2(S1): S92–S97.
[12] Johnson D R, Inui H, Muto S, et al. Microstructural development during directional solidification of alpha-seeded TiAl alloys. Acta Materialia, 2006, 54(4): 1077–1085.
[13] Inui H, Oh M H, Nakamura A, et al. Room-temperature tensile deformation of polysynthetically twinned (PST) crystals of TiAl. Acta Metallurgica Materialia, 1992, 40(11): 3095–3104.
[14] Kishida K, Inui H, Yamaguchi M, et al. Deformation of PST crystals of a TiAl/Ti3Al two-phase alloy at 1000 °C. Intermetallics, 1999, 7(10): 1131–1139.
[15] Hou Z Y, Li Y S, Mei H J, et al. Lamellar morphology of directional solidified Ti-45Al-6Nb-xW alloys. Rare Metals, 2016, 35(1): 65–69.
[16] Chen G, Peng Y B, Zheng G, et al. Polysynthetic twinned TiAl single crystals for high-temperature applications. Nature Materials, 2016, 15(8): 876–881.
[17] Kartavykh A V, Asnis E A, Piskun N V, et al. A promising microstructure/deformability adjustment of β-stabilized γ-TiAl intermetallics. Materials Letters, 2016, 162: 180–184.
[18] Kartavykh A V, Asnis E A, Piskun N V, et al. Microstructure and mechanical properties control of γ-TiAl (Nb, Cr, Zr) intermetallic alloy by induction float zone processing. Journal of Alloys and Compounds, 2015, 643: S182–S186.
[19] Kartavykh A V, Asnis E A, Piskun N V, et al. Room-temperature tensile properties of float-zone processed β-stabilized γ-TiAl (Nb, Cr, Zr) intermetallic. Materials Letters, 2017, 188: 88–91.
[20] Kartavykh A V, Asnis E A, Piskun N V, et al. Complementary thermodynamic and dilatometric assessment of phase transformation pathway in new β-stabilized TiAl intermetallics. Materials Letters, 2017, 189: 217–220.
[21] Su Y Q, Liu T, Li X Z, et al. Lamellar orientation control in directionally solidified TiAl intermetallics. China Foundry, 2014, 11(4): 219–231.
[22] Kim M C, Oh M H, Lee J H, et al. Composition and growth rate effects in directionally solidified TiAl alloys. Materials Science & Engineering: A,1997, 240: 570–576.
[23] Jung I S, Jang H S, Oh M H, et al. Microstructure control of TiAl alloys containing β stabilizer by directional solidification. Materials Science & Engineering: A, 2002, 329: 13–18.
[24] Dong S L, Chen R R, Guo J J, et al. Effect of heat treatment on microstructure and mechanical properties of cast and directionally solidified high-Nb contained TiAl-based alloys. Journal of Materials Research, 2015, 30(21): 3331–3342.
[25] Jung I S, Oh M H, Park N J, et al. Lamellar boundary alignment of DS-processed TiAl-W alloys by a solidification procedure. Metals and Materials International, 2007, 13(6): 455–462.

[26] Xiao Z X, Zheng L J, Yang L L, et al. Effects of temperature gradient on lamellar orientations of directional solidified TiAl-based alloy. Acta Metallurgica Sinca, 2010, 46(10): 1223–1229. (In Chinese)
[27] Xiao Z X, Zheng L J, Yan J, et al. Lamellar orientations and growth directions of β dendritics in directionally solidified Ti-47Al-2Cr-2Nb alloy. Journal of Crystal Growth, 2011, 324(1): 309–313.
[28] Fan J L, Li X Z, Su Y Q, et al. Dependency of microstructure parameters and microhardness on the temperature gradient for directionally solidified Ti-49Al alloy. Materials Chemistry and Physics, 2011, 130(3): 1232–1238.
[29] Fan J L, Li X Z, Su Y Q, et al. The microstructure parameters and microhardness of directionally solidified Ti-43Al-3Si alloy. Journal of Alloys and Compounds, 2010, 506(2): 593–599.
[30] Cadirli E, Kaya H, Gunduz M. Effect of growth rates and temperature gradients on the lamellar spacing and the undercooling in the directionally solidified Pd-Cd eutectic alloy. Materials Research Bulletin, 2003, 38(9–10): 1457–1476.
[31] Boyuk U, Marasli N, Kaya H, et al. Directional solidification of Al-Cu-Ag alloy. Applied Physics A, 2009, 95(3): 923–932.
[32] Zhong H, Li S M, Kou H C, et al. The solidification path related columnar-to-equiaxed transition in Ti-Al alloys. Intermetallics, 2015, 59: 81–86.
[33] Chen G L, Xu X J, Teng Z K, et al. Micro segregation in high Nb containing TiAl alloy ingots beyond laboratory scale. Intermetallics, 2007, 15(5-6): 625–631.
[34] Kaya H, Cadirli E, Gunduz M. Directional cellular growth of Al-2wt.% Li bulk samples. Applied Physics A, 2009, 94(1): 155–165.
[35] Ding X F, Lin J P, Zhang L Q, et al. Microstructure development during directional solidification of Ti-45Al-8Nb alloy. Journal of Alloys and Compounds, 2010, 506(1): 115–119.
[36] Zhang Y, Li X Z, Guo J J, et al. Effect of growth rate on characteristic lengths of microstructure in directionally solidified Ti-46Al-2Cr-2Nb-0.2B alloy. China Foundry, 2013, 10(5): 304–309.
[37] Lapin J, Ondrúš L, Nazmy M. Directional solidification of intermetallic Ti-46Al-2W-0.5Si alloy in alumina moulds. Inermetallics, 2002,10(10): 1019–1031.
[38] Dimiduk D M, Hazzledine P M, Parthasarathy T A. The role of grain size and selected microstructural parameters in strengthening fully lamellar TiAl alloys. Metallurgical Materials Transactions A, 1998, 29(01): 37–47.
[39] Kaya H, Gündüz M, Cadirli E, et al. Dependency of microindentation hardness on solidification processing parameters and cellular spacing in the directionally solidified Al based alloys. Journal of Alloys and Compounds, 2009, 478(1–2): 281–286.
[40] Liu G H, Zhang Y, Li X Z, et al. Effect of growth rate on microstructure evolution and hardness in directionally solidified Ti-50Al-6Nb. Rare Metal Materials and Engineering, 2015, 44(7): 1655–1660.